AGU PUBLICATIONS

JGR

Journal of Geophysical Research: Atmospheres

RESEARCH ARTICLE
10.1002/2013JD020930

Key Points:
- First Svalbard δ^{15}N and δ^{18}O ice core records
- Ice core δ^{15}N reflects fossil fuel combustion, soil emissions, and forest fires

Correspondence to:
C. P. Vega,
carmen.vega@geo.uu.se

Citation:
Vega, C. P., V. A. Pohjola, D. Samyn, R. Pettersson, E. Isaksson, M. P. Björkman, T. Martma, A. Marca, and J. Kaiser (2015), First ice core records of NO_3^- stable isotopes from Lomonosovfonna, Svalbard, *J. Geophys. Res. Atmos.*, *120*, 313–330, doi:10.1002/2013JD020930.

Received 25 SEP 2013
Accepted 6 DEC 2014
Accepted article online 11 DEC 2014
Published online 12 JAN 2015

First ice core records of NO_3^- stable isotopes from Lomonosovfonna, Svalbard

C. P. Vega[1], V. A. Pohjola[1], D. Samyn[1,2], R. Pettersson[1], E. Isaksson[3], M. P. Björkman[3,4], T. Martma[5], A. Marca[6], and J. Kaiser[6]

[1]Department of Earth Sciences, Uppsala University, Uppsala, Sweden, [2]Now at Department of Mechanical Engineering, Nagaoka University of Technology, Nagaoka, Japan, [3]Norwegian Polar Institute, Tromsø, Norway, [4]Now at Department of Earth Sciences, University of Gothenburg, Göteborg, Sweden, [5]Institute of Geology, Tallinn University of Technology, Tallinn, Estonia, [6]School of Environmental Sciences, University of East Anglia, Norwich, UK

Abstract Samples from two ice cores drilled at Lomonosovfonna, Svalbard, covering the period 1957–2009, and 1650–1995, respectively, were analyzed for NO_3^- concentrations, and NO_3^- stable isotopes (δ^{15}N and δ^{18}O). Post-1950 δ^{15}N has an average of (-6.9 ± 1.9)‰, which is lower than the isotopic signal known for Summit, Greenland but agrees with values observed in recent Svalbard snow and aerosol. Pre-1900 δ^{15}N has an average of (4.2 ± 1.6)‰ suggesting that natural sources, enriched in the ^{15}N isotope, dominated before industrialization. The post-1950 δ^{18}O average of (75.1 ± 4.1)‰ agrees with data from low and polar latitudes, suggesting similar atmospheric NO_y ($NO_y = NO + NO_2 + HNO_3$) processing pathways. The combination of anthropogenic source δ^{15}N and transport isotope effect was estimated as −29.1‰ for the last 60 years. This value is below the usual range of NO_x ($NO_x = NO + NO_2$) anthropogenic sources which is likely the result of a transport isotope effect of −32‰. We suggest that the δ^{15}N recorded at Lomonosovfonna is influenced mainly by fossil fuel combustion, soil emissions, and forest fires; the first and second being responsible for the marked decrease in δ^{15}N observed in the post-1950s record with soil emissions being associated to the decreasing trend in δ^{15}N observed up to present time, and the third being responsible for the sharp increase of δ^{15}N around 2000.

1. Introduction

The atmospheric reactive nitrogen (N_r) load has increased as a consequence of human activities [*Mosier et al.*, 2002]. N_r can alter the atmosphere, cryosphere, hydrosphere, and marine and terrestrial ecosystems as it transforms along pathways in the biochemical cycle, in a way that has been described as the "nitrogen cascade" [*Galloway et al.*, 2003]. Airborne nitrogen species are easily transported over meso- (10^2 km) and large- (10^3 km) spatial scales [*Holland et al.*, 1999] and the increase in the long-range atmospheric transport of N_r from low to high latitudes is thought to have generated a concentration increase in the Arctic environment [*Mayewski et al.*, 1990; *Laj et al.*, 1992; *Fischer et al.*, 1998; *Goto-Azuma and Koerner*, 2001; *Kekonen et al.*, 2002; *Burkhart et al.*, 2006]. Chemical analyses of ice cores have shown a twofold increase in nitrogen deposition in Greenland during the last 100 years [*Laj et al.*, 1992; *Fischer et al.*, 1998; *Burkhart et al.*, 2006] and in Svalbard since the midtwentieth century [*Goto-Azuma and Koerner*, 2001; *Kekonen et al.*, 2002]. Nitrate (NO_3^-) concentrations reached a maximum during the mid-1970s at Svalbard, followed by a decrease between the mid-1980s and late-1990s [*Samyn et al.*, 2012] in agreement with N_r emission trends [*Lamarque et al.*, 2010]. Due to its remote and relative pristine location, the Arctic has very fragile nitrogen-limited ecosystems that can be altered by relatively small increases of dry or wet deposition of N_r [*Shaver and Chapin*, 1980; *Atkin*, 1996; *Aanes et al.*, 2000; *Dickson*, 2000; *Rinnan et al.*, 2007].

Various studies have been undertaken to trace NO_x ($NO_x = NO_2 + NO$) sources and sinks in the Arctic [*Jarvis et al.*, 2008; *Morin et al.*, 2008]. These studies have often focused on the processes occurring in the snowpack involving NO_x, NO_3^-, and NO_2^- transformations [*Honrath et al.*, 2000; *Beine et al.*, 2002]. Since NO_3^- is the final oxidation product of NO_x, its concentration measured in ice cores could potentially be used as a proxy of NO_x emissions [*Kekonen et al.*, 2002; *Hastings et al.*, 2004, 2009]. However, postdepositional effects must be considered for its interpretation [*Röthlisberger et al.*, 2002]. Measurements of the nitrogen isotope delta of NO_3^-, found in the atmosphere could be used to identify NO_x sources, since δ^{15}N is thought not to change significantly during NO_x oxidation [*Moore*, 1977], although exchange between NO_x and NO_y

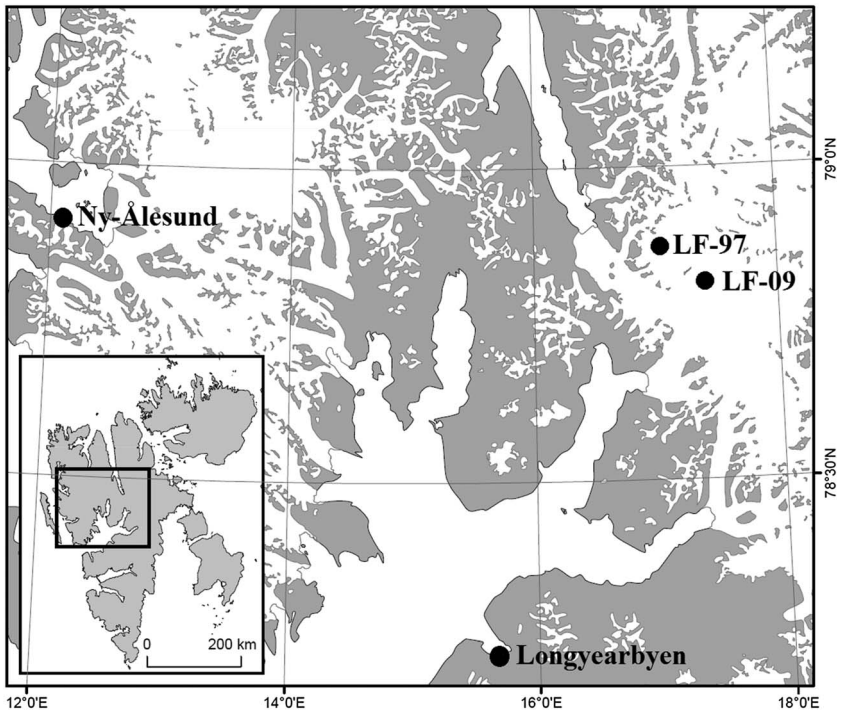

Figure 1. Map of Svalbard showing the Lomonosovfonna 2009 and 1997 ice core drilling sites in central Spitsbergen. Ny-Ålesund, central-west Spitsbergen, where snow [*Heaton et al*., 2004] and atmospheric nitrogen data [*Aas et al*., 2011] used in this work were sampled and recorded.

($NO_y = NO + NO_2 + HNO_3 +$ other nitrogen oxidation products) species affects the nitrogen isotope delta of the final NO_3^- [*Begun and Melton*, 1956; *Brown and Begun*, 1959]. Additional measurements of the $^{18}O/^{16}O$ and $^{17}O/^{16}O$ isotope delta in the NO_3^- molecule reflect the oxidative path of NO_3^- formation [*Michalski et al*., 2003]. This allows characterizing the seasonal variability in NO_3^- production pathways in the Arctic [*Morin et al*., 2008].

NO_3^- data from different ice cores drilled in Svalbard (Snøfjellafonna, Vestfonna, Austfonna, and Lomonosovfonna) show that NO_3^- concentrations increased 3–4 times over this region between 1950 and the late-1960s with a subsequent decrease since the late-1970s in Snøfjellafonna and Vestfonna [*Goto-Azuma et al*., 1995; *Goto-Azuma and Koerner*, 2001; *Samyn et al*., 2012]. A similar trend was observed in a Lomonosovfonna ice core drilled in 1997 [*Kekonen et al*., 2002; *Samyn et al*., 2012] showing a sharp increase starting in the 1950s, reaching maximum values during the 1970s and then a rapid decrease between the mid-1980s and 1997, behavior which is consistent with global N_r emission trends [*Lamarque et al*., 2010].

In this study, we present combined measurements of stable N and O isotopic ratios of NO_3^- in two ice cores drilled at Lomonosovfonna, Svalbard, in 1997 and 2009, covering the period from 1650 to 2009. This is the first of such records to be developed from the Norwegian Arctic. We use our measurements to estimate anthropogenic contributions to NO_3^- inputs to this sector of the Arctic and discuss potential processes that may affect the isotopic record either during air transport, deposition, or postdeposition. We also compare the Lomonosovfonna ice core record of NO_3^- deposition with time series of atmospheric concentrations of nitric acid (HNO_3), aerosol NO_3^- ($NO_{3(p)}^-$), and NO_3^- in precipitation ($NO_{3(aq)}^-$), measured at Zeppelin Mountain, in Ny-Ålesund, Svalbard [*Aas et al*., 2011].

2. Study Site and Methods

The Svalbard archipelago is located between 74°and 80°N, and between 10° and 35°E (Figure 1). It is positioned in a geographical area that experiences high climatic variations over the year. Polluted air masses from

central Europe, Scandinavia and north western Russia reach Svalbard during winter [*Stohl*, 2006; *Hirdman et al*., 2010]. Furthermore, circumpolar circulation patterns transport polluted air masses from Eastern North America across Iceland, but when these air masses reach Svalbard, their pollutant concentrations are significantly depleted due to precipitation over the ocean [*Barrie*, 1986]. According to a 10 year climatology of long-range atmospheric transport to Ny-Ålesund, Svalbard (Figure 1), eight major transport patterns were identified to arrive at Ny-Ålesund [*Eneroth et al*., 2003]. These transport patterns were clustered in two groups: (a) transport across the Arctic Basin and (b) transport originated from Eurasia and the Atlantic. During spring and summer, stable weather conditions and low cyclonic activity produce stagnant flow regimes and the air masses remain mostly confined to the Arctic Basin (a); while during autumn and winter, intense cyclonic activity dominates and air masses are transported from Eastern North America, North Atlantic, Northern Europe, and Eurasia (b).

The average snow accumulation rate at Lomonosovfonna has been estimated as (0.2 ± 0.1) m a^{-1} w.e. (meters water equivalent per year) between the eighteenth century and the first half of the twentieth century, and as (0.4 ± 0.1) m a^{-1} w.e. in the second half of the twentieth century [*V. Pohjola et al*., 2002].

Two parallel ice cores, LF-09 (37 m depth) and LF-09_{deep} (150 m depth), were drilled in 2009 at Lomonosovfonna, Svalbard (78°49′24"N, 17°25′59"E, and 1200 m asl (above sea level)) by a Norwegian-Swiss-Swedish ice drilling expedition [*Wendl et al*., 2011] (Figure 1). In addition, samples from an ice core drilled in 1997 (LF-97, 121 m depth) [*Isaksson et al*., 2001] were also analyzed for NO_3^- concentrations and NO_3^- stable isotopes. The LF-97 ice core was drilled 4.5 km north of the LF-09 site and has been widely published. Of the two parallel ice cores drilled in 2009, NO_3^- isotopologues were only measured in the shorter LF-09 ice core. In addition, 24 samples of the LF-97 ice core [*Isaksson et al*., 2001] were analyzed for NO_3^- isotopologues. These LF-97 samples were collected from the remaining ice, which had been kept frozen at −20°C since 1997, and represent an estimated time span between 1652 and 1995 [*Isaksson et al*., 2001; *Divine et al*., 2011]. In order to minimize contamination of the ice and firn samples during preparation and analyses, all the materials used (bags, cutting tools, tubes, and bottles) were rinsed with ultrapure water (18 MΩ cm). Disposable polyethylene powder free gloves, particle masks, and clean overalls were worn during cutting and analyses. The LF-09 ice core subsections (the average length of each subcore was (62 ± 12) cm) were measured, photographed, and weighed in the cold room at the Norwegian Polar Institute, Tromsø, Norway, while the cutting of the LF-97 samples was done at the Department of Earth Sciences, Uppsala University, Sweden. The cleaning and cutting of the firn and ice subcores were done using a stainless steel band saw and table, which were cleaned at least 5 times with acetone (Merck) before cutting. To ensure the cleanness of the cutting table and saw, blank ice blocks were cut and sampled before processing the ice core.

The samples to be analyzed for major ions and for N and O isotope ratios of NO_3^- were taken from 1/8 of the ice core area (the ice core has 8 cm of diameter). About 1–2 cm were removed from the outer part of each core section to prevent any contamination caused by the drill, storage, and handling; the drilling process was done without using any fluid. Blocks of 1.8 cm side × 1 cm side × 8 cm long were used for ions and, 4 cm side × 1 cm side × length of each subcore blocks were used for NO_3^- stable isotopes. Major ions (Na^+, NH_4^+, K^+, Ca^{2+}, Mg^{2+}, F^-, Cl^-, Br^-, NO_3^-, and SO_4^{2-}) were analyzed using a ProfIC850 Metrohm ion chromatograph with isocratic eluent flow at the Department of Earth Sciences, Uppsala University, Sweden. NO_3^- stable isotopes were analyzed using the denitrifier method at the School of Environmental Sciences, University of East Anglia, UK [*Casciotti et al*., 2002; *Kaiser et al*., 2007]. The nitrogen and oxygen isotopic composition of the NO_3^- are expressed as delta values $\delta^{15}N$ (in International Union of Pure and Applied Chemistry (IUPAC) nomenclature written as $\delta(^{15}N, ^{14}N, NO_3^-)$), and $\delta^{18}O$ (in IUPAC nomenclature written as $\delta(^{18}O, ^{16}O, NO_3^-)$) in per mill (‰), relative to an international standard, following

$$\delta = \frac{R_{\text{sample}} - R_{\text{standard}}}{R_{\text{standard}}} \quad (1)$$

where R represents the ratio $^{15}N/^{14}N$ or $^{18}O/^{16}O$ in the sample and in the standard, respectively. The $\delta^{15}N$ and $\delta^{18}O$ values were expressed relative to Air-N_2 (N_2 in atmospheric air) and VSMOW (Vienna Standard Mean Ocean Water), respectively. According to equation (1), negative delta values mean depletion in the heavier isotope; positive delta values mean enrichment, with respect to the standard.

For the isotope analyses, one sample for each subsection of the LF-09 ice core was collected in clean high-density polyethylene plastic bottles, resulting in 31 samples covering a depth between 0 and 19.4 m, and 20 samples

Table 1. Stable NO_3^- Isotopes Percentages and NO_3^- Concentrations Measured in the Six Test Samples, Before and After Freeze Drying

	Before Freeze Drying			After Freeze Drying			
Sample	$\delta^{15}N$ (‰)	$\delta^{18}O$ (‰)	NO_3^- (μmol L^{-1})	$\delta^{15}N$ (‰)	$\delta^{18}O$ (‰)	NO_3^- (μmol L^{-1})	Preconcentration factor NO_3^-
S1	6.97	43.53	7.51	7.17	43.54	35.22	5
S2	7.22	43.42	8.19	7.31	43.08	71.63	9
S3	6.89	43.62	8.3	7.31	43.06	110.43	13
S4	7.14	44.09	8.02	7.34	43.01	47.9	6
S5	7.09	43.62	8.06	7.29	43.25	39.63	5
S6	7.12	43.56	8.13	7.35	43.11	79.63	10

between 24.0 and 36.3 m. The ice core section between 19.4 and 24.0 m depth was sampled at 10 cm resolution, resulting in 45 samples. The samples were melted at room temperature under a laminar flow cabinet (class 100), and 10 mL of sample were collected in clean plastic tubes to analyze the NO_3^- concentrations using ion chromatography. The NO_3^- isotopic measurements using the denitrifier method employing *Pseudomonas aureofaciens* denitrifying bacteria for the NO_3^- to N_2O conversion [*Casciotti et al*., 2002; *Kaiser et al*., 2007] requires a minimum of 10 nmol of nitrate (20 nmol being optimum) in at most 13 mL of sample. For this reason, all samples with $NO_3^- < 1\ \mu mol\ L^{-1}$ were concentrated using lyophilization (freeze drying the samples until a final volume of about 10 mL) until they reached a concentration $> 1\ \mu mol\ L^{-1}$. Only eight samples were too low in concentration after freeze drying, to be analyzed. All samples were filtered using 0.2 μm syringe filters (Minisart PES), collected in clean plastic tubes, and kept frozen until isotopic analysis.

To determine how the lyophilization process may affect $\delta^{15}N$ and $\delta^{18}O$ in ice cores, six bulk surface snow samples taken on 8 May 2010 at Austre Brøggerbreen, Ny-Ålesund, were used as test. The concentrations and isotopic composition of NO_3^- in these samples were measured before and after freeze drying (Table 1).

It was found that there is a linear correlation ($r = 0.60$) between the differences in $\delta^{15}N$ and the concentration factor resulting from freeze drying. A concentration factor of 10 led to a 0.33‰ increase of $\delta^{15}N$. Low correlation was found ($r = -0.14$) between the differences in $\delta^{18}O$ and the concentration factor, after and before freeze drying.

Considering that the observed range of $\delta^{15}N$ in the LF-09 ice core is about 15‰ and that the concentration factors for most of the lyophilized LF-09 samples were < 10, the changes in $\delta^{15}N$ due to sample preconcentration are negligible compared to the environmental variability and can be disregarded.

The $\delta^{15}N$ values measured in the ice cores were not corrected for the contribution of $N_2{}^{17}O$ to *m/z* 45 during isotope ratio mass-spectrometric analysis (^{17}O excess or $\Delta^{17}O$) [*Coplen et al*., 2004]. Since $\delta^{17}O$ (IUPAC nomenclature written as $\delta(^{17}O, ^{16}O, NO_3^-)$) usually correlates well with $\delta^{18}O$, we estimate that the true $\delta^{15}N$ is probably 1–2‰ lower than the values presented here. Second-order variations in the correlation between $\delta^{17}O$ and $\delta^{18}O$ depending on season and meteoric water composition influences have been reported by *Morin et al*. [2008]. Considering any given $\delta^{18}O$ value, a variation of $\Delta^{17}O$ in the order of at most 6‰ is expected [*Morin et al*., 2008], resulting in variations in the $\delta^{15}N$ downward correction of at most 0.3‰, which can be considered negligible. Considering that the focus of this study is on trends in the stable isotope composition rather than absolute values, we show $\delta^{15}N$ values without $\delta^{17}O$ correction.

Since no corrections for lyophilization and for the contribution of $N_2{}^{17}O$ to *m/z* 45 during isotope ratio mass-spectrometric analysis were applied to the data, our values are biased toward higher $\delta^{15}N$ by, on average, 1.5‰ and, at most, by 2.3‰.

3. Dating of the LF-09 Ice Core

To estimate the time interval covered by the LF-09 ice core, the $\delta^{18}O$-H_2O (in IUPAC nomenclature written as $\delta(^{18}O, ^{16}O, H_2O)$, expressed as relative isotope ratio difference to Vienna Standard Mean Ocean Water (VSMOW)), values from the top 30 m of the LF-09_{deep} ice core [*Wendl et al*., 2011] were used to count annual cycles. An automatic cycle-counting routine [*V. A. Pohjola et al*., 2002] was used to minimize subjective errors

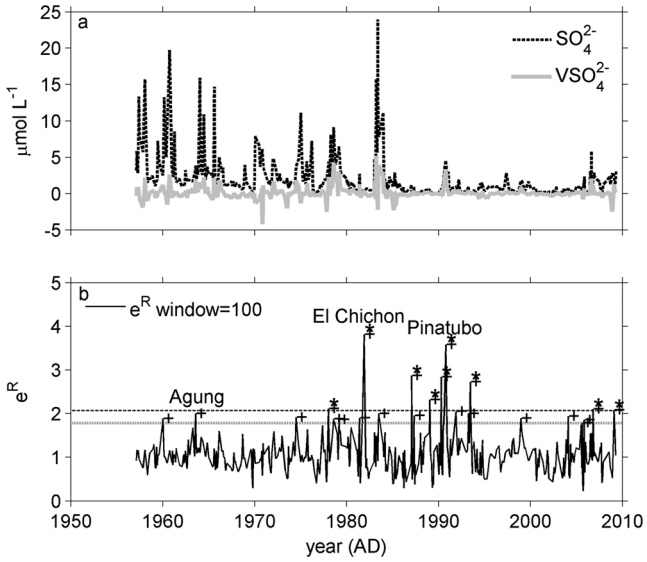

Figure 2. (a) Total sulfate (SO_4^{2-}, black dashed line) and volcanic sulfate (VSO_4^{2-}, grey line) in µmol L^{-1} measured in the LF-09 ice core as function of time. (b) Ratio of the measured sulfate relative to the model fit (e^R) [*Moore et al.*, 2012], grey and black dashed lines indicate the confidence interval at 95% and 99%, respectively. Three volcanic horizons were selected as possible candidates (e^R over the 95% confidence interval and VEI > 4): Agung (1963), El Chichón (1982), and Pinatubo (1991) were used to constrain the time scale obtained by using automated δ^{18}O-H_2O cycle counting.

that could be associated with manual cycles counting. The routine counts δ^{18}O-H_2O cycles that fulfill two criteria: (1) having amplitude > 0.1‰ and (2) subannual snow accumulation between 0.05 and 0.33 m w.e. Using these two criteria and a tritium horizon found at 23.6 m w.e. in the LF-09$_{deep}$ ice core [*Wendl et al.*, 2011], which is a result of past nuclear tests and assumed to peak in 1963 [*Pinglot et al.*, 2003; *van der Wel et al.*, 2011], we were able to date the LF-09 ice core. The results were compared with a first dating attempt for the top 30 m deep of the LF-09$_{deep}$ ice core done by manual δ^{18}O-H_2O cycles counting [*Wendl et al.*, 2011]. In addition to δ^{18}O-H_2O cycles counting, a multilinear regression model [*Moore et al.*, 2012] constructed using chemical data (major ions) to model the total sulfate present in the ice core was used to extract the volcanic sulfate portion (VSO_4^{2-}) by calculating the model residuals (e^R) [*Moore et al.*, 2012]. By using this method, it was possible to identify potential volcanic horizons in the LF-09 sulfate record, which were used to further constrain the time scale. Figure 2 shows the residuals of the multilinear regression model when Na^+, Cl^-, NO_3^-, and Mg^{2+} concentrations were used as inputs to the model, and a window of 100 points (from a total of 444 samples) was used. Only the peaks found with a 99% significance level were considered to assign a possible volcanic eruption (with the exception of the peak associated with the Agung volcanic eruption found at 22.97 m w.e.). Only relatively local and equatorial eruptions with a Volcanic Explosivity Index (VEI) higher than 4, listed in the Global Volcanism Program (2013, http://www.volcano.si.edu/index.cfm), were considered as possible sulfate horizon candidates. Three volcanic horizons were selected as possible candidates (e^R over the 95% confidence interval and VEI > 4): Agung (eruption 1963, confirmed by the tritium signal [*Wendl et al.*, 2011]), El Chichón (eruption 1982), and Pinatubo (eruption 1991), and were used to constrain the time scale obtained with the automatic δ^{18}O-H_2O cycles counting (Figure 3).

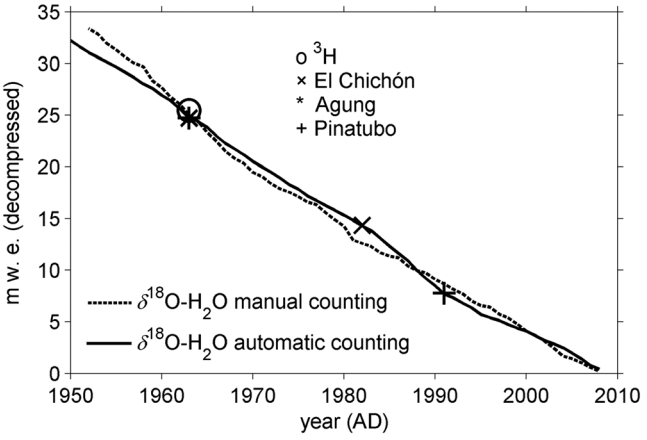

Figure 3. Comparison between time scales obtained by manual [*Wendl et al.*, 2011] and automated δ^{18}O-H_2O cycle-counting methods, black dashed and solid lines, respectively. Both countings were done considering the winter minima in the δ^{18}O-H_2O record and bottom depths. The manual counting was done down to 23.6 m w.e., where the tritium peak (open circle) was identified in the LF-09$_{deep}$ ice core [*Wendl et al.*, 2011]. The Agung (asterisk), El Chichón (cross), and Pinatubo (plus) volcanic eruptions found in the sulfate LF-09 ice core data were used to constrain the time scale obtained by using the automated δ^{18}O-H_2O cycle counting.

By using these different independent dating methods, the LF-09 core was estimated to cover a span of 52 years between 1957 and 2009.

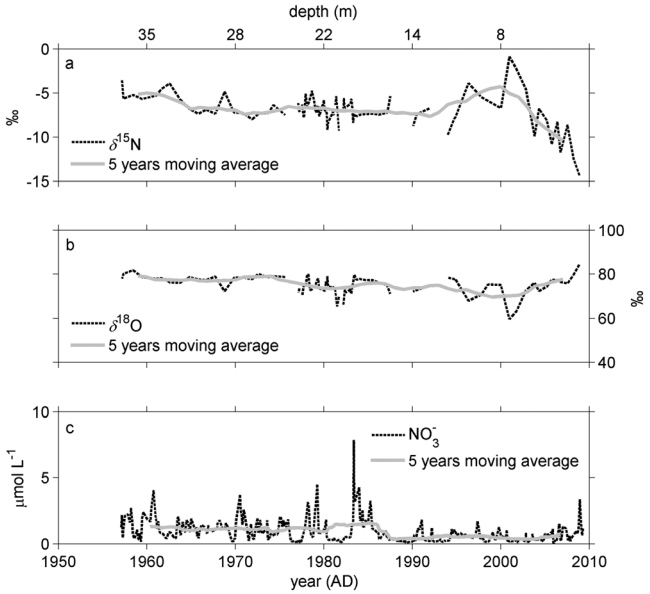

Figure 4. (a) The δ^{15}N measured in the LF-09 ice core (dashed line) and 5 year moving average (grey line), as function of depth (top axis) and time (bottom axis). (b) The δ^{18}O measured in the LF-09 ice core (dashed line) and 5 year moving average (grey line), as function of depth and time. (c) NO_3^- concentrations in µmol L^{-1} measured in the LF-09 ice core (dashed line) and 5 year moving average (grey line), as function of depth and time.

The average temporal resolution for each ice core sample of NO_3^- isotopes is ≈ 0.9 years. Considering that the melt index (defined as the ratio between ice affected and not affected by melting) of an earlier ice core, LF-97, drilled ≈ 4.5 km NE from the LF-09 drilling site, was estimated as 55% [*V. A. Pohjola et al.*, 2002], the isotope deltas and major ion data presented here were smoothed with moving average windows of 5 and 50 points (≈ 5 years), respectively, to minimize potential artifacts in the annual isotopic record caused by percolation and refreezing of melt water.

4. Results

We have divided our data sets in two periods: post-1950 and pre-1950. The period post-1950 is covered by the LF-09 ice core entirely and reflects industrialized times. On the other hand, the period pre-1950 contains data from the LF-97 ice core between 1650 until 1950 and covers both preindustrial and industrial times. Further in section 5.2 we refer to preindustrial sources as pre-1900 values. This temporal separation has been followed in this study considering the global fossil fuel combustion emission increase observed after 1900 [*van Aardenne et al.*, 2001].

4.1. Post-1950 Period

The results of the LF-09 NO_3^- stable isotopes and NO_3^- concentrations are shown in Figure 4. All LF-09 δ^{15}N values were found to be negative with an average value of (-6.9 ± 1.9) ‰, which is in contrast to the observations in post-1950 Greenland ice [*Freyer et al.*, 1996; *Hastings et al.*, 2004, 2009], where the δ^{15}N average was (0.5 ± 2.4)‰ (Table 2). Despite this difference, the LF-09 δ^{15}N values are in the same range of the fall and winter surface snow values registered at Summit, Greenland, in 2000 [*Hastings et al.*, 2004].

The δ^{15}N shows a slightly decreasing trend from values of about −3.5‰ at the bottom of the ice core, dated to be 1957, to −8.0‰ at a depth of 25 m, dated to be the mid-1970s. The δ^{15}N remained stable between 25 m to 12 m deep, in the time scale being estimated as the mid-1970s and early 1990s. A rapid increase in δ^{15}N is observed between 12 m to 7.5 m deep, estimated to be the mid-1990s until 2001, when δ^{15}N reached the maximum value of −0.9‰ during the whole length of the LF-09 record, decreasing rapidly afterward to a minimum value (−14.4‰) in the uppermost meter of the ice core, dated as 2009. The δ^{18}O values are stable between the bottom of the ice core to 25 m deep (from late 1950s to mid-1970s), with mean values close to 80.0‰ and show a decreasing trend afterward, reaching a minimum of 59.7‰ at 7.5 m deep (2001). After this minimum, the δ^{18}O increases again reaching pre-1980s levels (Figure 4).

NO_3^- concentrations were relatively steady and high between 36 m and 15 m deep, estimated as late-1950s and late-1980s with an average of 1.2 µmol L^{-1}. Between 15 m deep and the top of the ice core, the average NO_3^- concentrations dropped to half the amount registered in the previous period (Figure 4) which is in accordance with the NO_3^- trends found in the LF-97 ice core [*Kekonen et al.*, 2002; *Samyn et al.*, 2012] and with NO_x emission estimates [*van Aardenne et al.*, 2001; *EC-JRC/PBL. EDGAR version 4.2*, 2011].

Table 2. Average Values of $\delta^{15}N$, $\delta^{18}O$, and NO_3^- Measured in the LF-09 Ice Core, Fresh Snow From Ny-Ålesund, Ny-Ålesund Aerosol Data, and in Snow and Ice Cores From Greenland and the Alps

Site	NO_3^- (μmol L^{-1})	$\delta^{15}N$[a] (‰)	$\delta^{18}O$ (‰)
LF-09 [this study]	0.9 ± 0.8	−6.9 ± 1.9	75.1 ± 4.1
LF-97 [this study] pre-1900	0.6 ± 0.2	4.2 ± 1.6	66.2 ± 5.7
Fresh snow Ny-Ålesund[c]			
Feb 2010	2.9 ± 0.2	−14.6 ± 0.2	79.2 ± 0.6
Apr 2010	1.0 ± 0.2	−13.9 ± 1.1	83.0 ± 4.0
Apr 2010	1.6 ± 0.1	−18.6 ± 0.8	86.0 ± 1.2
Apr 2010	1.5 ± 0.1	−13.3 ± 0.4	82.8 ± 1.0
Fresh snow Ny-Ålesund[b]			
Apr 2001	2	−17.8	68.2
Apr 2002	4	−8.6	70.8
Aerosol Ny-Ålesund[d]			
Feb–Apr 2006		−15 ± 4	87 ± 4
Summit Greenland-snow[f]			
Fall 2000	1.6 ± 0.7	−9.2 ± 5.4	74.6 ± 1.8
Winter 2000–2001	2.0 ± 0.7	−10.0 ± 3.2	77.5 ± 2.4
Spring 2001	1.7 ± 0.4	−1.4 ± 3.0	75.4 ± 1.9
Summer 2001	2.8 ± 1.5	−0.8 ± 5.3	68.9 ± 2.1
Summit Greenland ice core[g]			
Pre-1850	1.2 ± 0.2	+11.4 ± 1.3	
Post-1950	2.1 ± 0.4	+0.5 ± 2.4	
Summit Greenland ice core[e]			
Pre-1950		+12 to +18	
Post-1950		−5 to +5	
Col du Dôme[e]			
Spring 1991/1992		−1.90	
Summer 1990		−4.46	
Summer 1991		−5.07 and −3.68	
Winter 1990/1992		−0.15	

[a]Since no corrections for lyophilization and for the contribution of $N_2{}^{17}O$ to *m/z* 45 during isotope ratio mass-spectrometric analysis were done to our data sets, our values are biased toward higher $\delta^{15}N$ with a maximum difference of ≈ 2.3‰ between the measured and the real value.
[b]*Heaton et al.* [2004].
[c]*Björkman* [2013].
[d]*Morin et al.* [2009].
[e]*Freyer et al.* [1996].
[f]*Hastings et al.* [2004].
[g]*Hastings et al.* [2009].

4.2. Pre-1950 Period

Figure 5 shows the NO_3^- stable isotopic results of the LF-97 ice core. The $\delta^{15}N$ values remained stable between 1650 and late 1800s, with a mean of (4.2 ± 1.6)‰ ($N = 18$). A decreasing trend is observed since late 1800s until 1995, with a mean of (−4.6 ± 4.5)‰ ($N = 6$), which agrees with the negative values found in the LF-09 ice core for the post-1950 period. The $\delta^{18}O$ values were stable for the covered period, with a mean of (64.9 ± 8.0)‰ which is much lower than the values observed during the post-1950 period. LF-97 $\delta^{15}N$ results show a decreasing trend similar to the one reported for Greenland [*Hastings et al.*, 2009]. This indicates that the transition from natural sources (e.g., lightning, soil emissions, and forest fires) during preindustrial times, toward a combination of natural and anthropogenic sources observed at Greenland [*Hastings et al.*, 2009] is also registered over Svalbard, but with an offset in the $\delta^{15}N$ values of about −7‰ compared to the Greenland record. Because our preindustrial data is scarce, we cannot tell if the $\delta^{15}N$ values present this offset over the whole period covered by both LF-97 and LF-09 ice cores or if this is just a lower boundary of the ice core $\delta^{15}N$ record.

NO_3^- concentrations were relatively steady and low between 1650 and 1900, with an average of (0.61 ± 0.24) μmol L^{-1}. For the samples between 1900 and 1995, the average was (0.61 ± 0.18) μmol L^{-1}. A comparison between the LF-97 samples previously reported [*Isaksson et al.*, 2001; *Kekonen et al.*, 2002] and the ones reanalyzed in this work is shown in Figure 6, where it can be observed that both data sets are

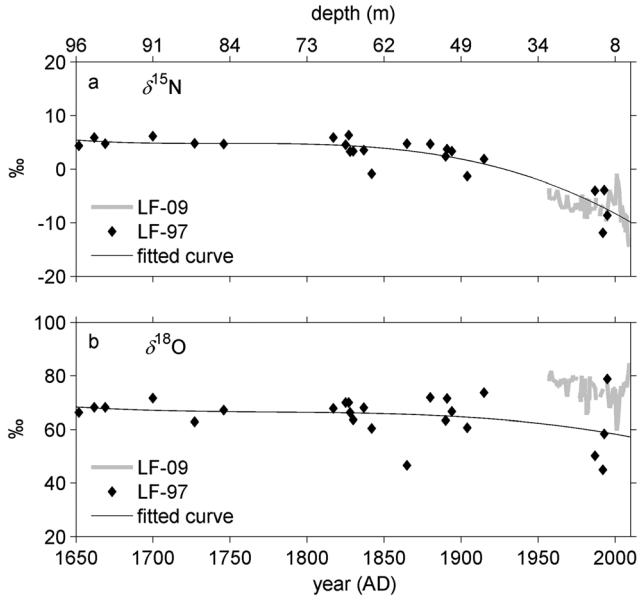

Figure 5. (a) The δ^{15}N found in the LF-97 ice core (black diamond), and a third-order polynomial fit to the data (black line), as function of depth (top axis) and time (bottom axis); δ^{15}N found in the LF-09 ice core as function of time is also shown (grey line). (b) Similar labels as in Figure 5a but for δ^{18}O.

comparable. This makes us conclude that the NO_3^- data have not been altered by 15 years of storage and that there is no methodological uncertainty biasing our LF-97 data.

5. Discussion

5.1. Postdepositional Effects on the NO_3^- Record

It is known that NO_3^- in the snow suffers postdepositional loss by photolysis and desorption of HNO_3 [*Honrath et al.*, 1999; *Dibb et al.*, 2002; *Röthlisberger et al.*, 2002], but these effects lead to an increase in the snow δ^{15}N values since the lighter molecules are more easily removed from the snow. It has been demonstrated that NO_x are emitted when snow is irradiated [*Honrath et al.*, 1999; *Honrath et al.*, 2000; *Dibb et al.*, 2002; *Hastings et al.*, 2004; *Jarvis et al.*, 2008], and such processes have been registered at Summit, Greenland, where postdepositional loss of NO_3^- has been found [*Honrath et al.*, 1999; *Dibb et al.*, 2002; *Röthlisberger et al.*, 2002; *Hastings et al.*, 2004]. However, a recent study by *Fibiger et al.* [2013] concludes that photolysis does not have a significant effect on snow NO_3^- concentration or isotope changes at Summit. Several investigations have also been made in Ny-Ålesund without confirming the importance of such processes for Svalbard [*Beine et al.*, 2003; *Amoroso et al.*, 2006; *Amoroso et al.*, 2010]. It remains uncertain whether photolysis significantly affects snow NO_3^- concentrations and isotopes at Lomonosovfonna. However, considering that postdepositional loss is only relevant at low-accumulation sites such as Antarctica or Greenland (mean annual accumulation of snow is (0.1435 ± 0.0035) m a^{-1} w.e. (assuming a snow density of 350 kg m^{-3}), during 1950–2000, and 0.097 m a^{-1} w.e. (assuming a snow density of 350 kg m^{-3}), during 1958–2003, for Antarctica and Greenland, respectively [*Arthern et al.*, 2006; *Hanna et al.*, 2006]), the average accumulation rate of (0.55 ± 0.1) m a^{-1} w.e. for the last 60 years at the LF-09 drilling site (Figure 7) does not support the hypothesis that postdepositional NO_3^- loss is relevant at Lomonosovfonna.

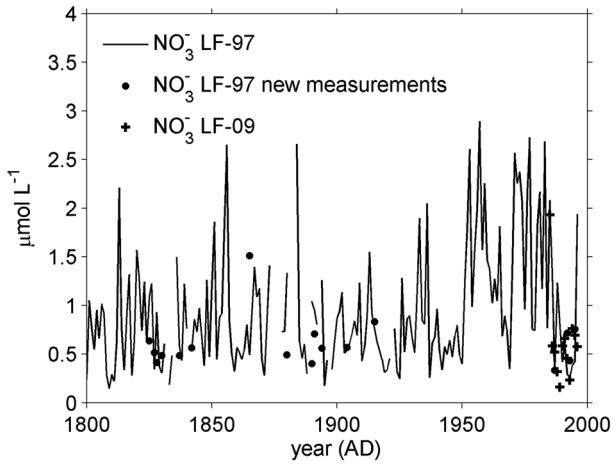

Figure 6. Comparison between the NO_3^- concentrations measured in the LF-97 ice core ~12 years ago [*Isaksson et al.*, 2001] (line) and the new measurements done in the remaining ice (black circle), compared with NO_3^- measured in the LF-09 ice core (plus).

NO_3^- produced by the oxidation of NO_x emitted from the snowpack shows δ^{15}N values of about −40‰ to −60‰ [*Freyer et al.*, 1996; *Wagenbach et al.*, 1998; *Savarino et al.*, 2007; *Morin et al.*, 2008; *Frey et al.*, 2009; *Savarino and Morin*, 2011], with NO_3^- photolysis being correlated with the snow-illumination index [*Morin et al.*, 2012]. This is at its maximum during springtime for polar regions, when snow is still present and the solar input is high,

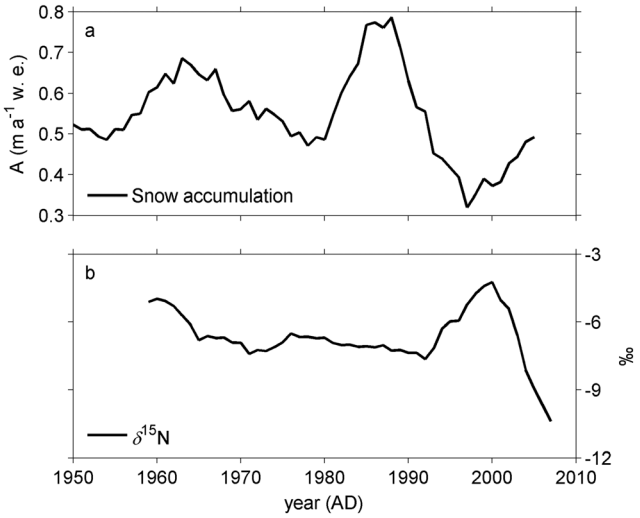

Figure 7. (a) Accumulation rate (*A*) calculated for the summit of Lomonosovfonna for the last 60 years and (b) the δ^{15}N values measured in the LF-09 ice core. All the series were smoothed using a 5 year moving average. The maximum value in the δ^{15}N record follows a decrease in the accumulations rates that reached a minimum around 1998.

but is close to zero during summer, when most of the land masses are free of snow (e.g., Arctic coastal sites and sea ice) [*Morin et al*., 2012]. Eastern Svalbard is largely covered with ice fields and ice caps, which could generate a permanent source of depleted δ^{15}N air masses when photolysis takes place during the illuminated part of the year. For instance, the isotopic LF-09 record could be influenced by the advection of air masses depleted in δ^{15}N produced by local snowpack photochemistry, which can be associated to the low δ^{15}N values observed in the record. To attribute the decreasing trend of δ^{15}N observed in the ice core during the last years to this local transport of depleted air masses would require a significant amount of precipitation or NO_3^- dry deposition during spring and summer in respect to the annual precipitation distribution. However, precipitation records of different Svalbard sites [*Førland et al*., 2011] indicate that most of the precipitation at Svalbard is registered during the winter and autumn seasons for the last decades and that dry deposition only accounts in average 14% of the total deposited NO_3^- in a central Svalbard glacier during 2009–2010 [*Björkman et al*., 2013]. Moreover, it has been registered that recent average spring-summer precipitation at Ny-Ålesund and Longyearbyen airport has been slightly lower than the reference period (1961–1990), while winter-autumn precipitation has increased [*Førland et al*., 2011]. Considering the previous and keeping in mind an average dry deposition effect on the order of the values reported by *Björkman et al*. [2013], it is unlikely that the decreasing trend observed in the ice core δ^{15}N could be produced by a local production, transport, and redeposition of photo-induced products carrying depleted δ^{15}N signatures.

5.2. Ice Core δ^{15}N and Possible Sources

The values of δ^{15}N from natural and anthropogenic sources vary within a vast range [*Li and Wang*, 2008; *Hastings*, 2010, and references therein; *Felix et al*., 2012]. The ice core results reported for Greenland [*Hastings et al*., 2009] revealed that high preindustrial δ^{15}N values, on the order of 9.0‰, point to a natural NO_x source that has a higher $^{15}N/^{14}N$ ratio than the sources described for present times [*Hastings*, 2010]. However, a recent study by *Erbland et al*. [2012] suggests that shifts of +18.7‰ in δ^{15}N detected at Summit, Greenland [*Hastings et al*., 2005] could be explained in terms of changes in nitrate postdepositional effects rather than pointing to a natural source of high $^{15}N/^{14}N$. Our preindustrial results (Figure 5a) show positive δ^{15}N values also in Svalbard but about 7‰ lower than in the Greenland record [*Hastings et al*., 2009]. This offset in δ^{15}N is observed along the whole LF-97 record and may be associated with differences in long-range atmospheric transport between Greenland and Svalbard [*Kahl et al*., 1997; *Eneroth et al*., 2003; *Stohl*, 2006]. At Summit, a 44 year climatology (1946–1989) show dominant source regions and transport routes located at East Asia (winter and spring), North America (summer), and the North Pacific (autumn) [*Kahl et al*., 1997]. While a different situation occurs at Svalbard, as mentioned in section 2, with stagnant flow regimes and air masses confined to the Arctic Basin (spring and summer) and transport from Eastern North America, North Atlantic, Northern Europe, and Eurasia, during autumn and winter [*Eneroth et al*., 2003]. If such transport conditions were prevalent during preindustrial times, a difference of 7‰ in δ^{15}N between the Greenland and Svalbard records might be a consequence of differences in NO_3^- source regions and strengths during preindustrial times. The influence of regions where agriculture was more extensive during preindustrial times (i.e., Europe compared to North America) on the LF-97 δ^{15}N record could be the explanation of such an offset, due to the low δ^{15}N values recently associated to soil emissions [*Li and Wang*, 2008].

Table 3. NO_x Source Emission Fraction of Combustion Sources (f_{comb}) and Soil Emissions (f_{soil}) of the United States, OECD Europe, and Russian Federation for the Period 1970–2008 [*EC-JRC/PBL. EDGAR version 4.2*, 2011, http://edgar.jrc.ec.europa.eu] and Average $\delta^{15}N_{ant}$ Based on Equation (6)

Row	Emission Fraction	United States	OECD Europe	Russian Federation	Source Delta $\delta^{15}N$ (‰)
1	f_{comb} (stationary + mobile sources)	0.9852	0.9748	0.9792	3.5[a]
2	f_{comb} (stationary sources)	0.2983	0.2438	0.4180	8.0[b]
3	f_{soil}	0.0148	0.0252	0.0208	−34.4[c]
4	$f_{comb}\delta_{comb}$ (stationary + mobile sources)	3.45	3.41	3.43	
5	$f_{comb}\delta_{comb}$ (stationary sources)	2.39	1.95	3.34	
6	$\delta^{15}N_{ant}$ (stationary + mobile sources)	2.94[d]	2.54[d]	2.71[d]	
7	$\delta^{15}N_{ant}$ (stationary sources)	5.99[d]	4.03[d]	5.99[d]	
8	$\delta^{15}N_{ant}(1+\varepsilon)+\varepsilon$ (equation (4))	−29.1	−29.1	−29.1	
9	Transport isotope effect ε based on rows 6 and 8 (stationary + mobile sources)	−31.94	−31.56	−31.73	
10	Based on rows 7 and 8 (stationary sources)	−34.89	−32.99	−34.88	

[a] *Hastings* [2010].
[b] *Felix et al.* [2012].
[c] *Li and Wang* [2008].
[d] This study.

A simple isotope-mass balance [*Freyer et al.*, 1996] was used to estimate the anthropogenic contribution ($\delta^{15}N_{ant}$) to the total ($_t$) nitrate concentration of $c_t(NO_3^-) = 0.9\ \mu mol\ L^{-1}$ with an isotope delta of $\delta^{15}N_{post\text{-}1950} = (-6.9 \pm 1.9)$ ‰ measured in the LF-09 ice core post-1950 (Table 2). The pre-1900 NO_3^- concentration of $c_{nat}(NO_3^-) = 0.6\ \mu mol\ L^{-1}$ with an isotope delta of $\delta^{15}N_{pre\text{-}1900} = (4.2 \pm 1.6)$‰ measured in the LF-97 ice core are assumed to represent natural sources. Designating the transport isotope effect as ε (equivalent to nonsource-related effects such as kinetic fractionation [*Freyer*, 1991]), the pre-1900 nitrate isotope delta is

$$\delta^{15}N_{pre-1900} = \delta^{15}N_{nat}(1+\varepsilon)+\varepsilon \tag{2}$$

where $\delta^{15}N_{nat}$ (and $\delta^{15}N_{ant}$) represent the isotopic composition at the source (before transport to Svalbard). The isotope delta post-1950 can be calculated as follows:

$$\begin{aligned}\delta^{15}N_{post\text{-}1950} &= f\left[\delta^{15}N_{nat}(1+\varepsilon)+\varepsilon\right] + (1-f)\left[\delta^{15}N_{ant}(1+\varepsilon)+\varepsilon\right] \\ &= f\delta^{15}N_{pre\text{-}1900} + (1-f)\left[\delta^{15}N_{ant}(1+\varepsilon)+\varepsilon\right]\end{aligned} \tag{3}$$

with $f = c_{nat}/c_t$. Equation (3) assumes that the transport isotope fractionation is the same for natural and anthropogenic sources. The sum of anthropogenic source delta and transport isotope effect can be calculated as follows:

$$\delta^{15}N_{ant}(1+\varepsilon)+\varepsilon = \frac{\delta^{15}N_{post\text{-}1950} - f\delta^{15}N_{pre\text{-}1900}}{1-f} \tag{4}$$

From equation (4), ε can be derived as follows:

$$\varepsilon = \frac{\frac{\delta^{15}N_{post\text{-}1950} - f\delta^{15}N_{pre\text{-}1900}}{1-f} - \delta^{15}N_{ant}}{1+\delta^{15}N_{ant}} \tag{5}$$

Consequently, $\delta^{15}N_{ant}$ can be calculated from the emission fraction weighted delta values of combustion and soil sources (f_{comb} and f_{soil}, respectively) (Table 3) as follows:

$$\delta^{15}N_{ant} = f_{comb}\delta^{15}N_{comb} + (1-f_{comb})\delta^{15}N_{soil} \tag{6}$$

using average $\delta^{15}N$ values [*Li and Wang*, 2008; *Hastings*, 2010; *Felix et al.*, 2012; this study] (Table 3) and source f_{comb} and f_{soil} (specific source NO_x emission/total NO_x emission) of the most relevant NO_x source regions to Svalbard (United States, OECD Europe, and Russian Federation) [*Samyn et al.*, 2012] (Table 3). The parameters f_{comb} and f_{soil} are the contributions of fossil fuel combustion and soil emissions to total emissions, based on average annual NO_x emissions between 1970 and 2008 [*EC-JRC/PBL. EDGAR version 4.2*, 2011 http://edgar.jrc.ec.europa.eu/] (Table 3).

Equation (4) gives a sum of anthropogenic source delta and transport isotope effect value (ε) of $-29.1‰$ for the last 60 years (Table 3). The calculated $\delta^{15}N_{ant}$ value is a combination of fossil fuel combustion emissions by automobiles and power plants ($\delta^{15}N$ ranges from -13 to 20‰, *Hastings* [2010, and references therein], and *Felix et al*. [2012]) and soil emissions, which have increased due to the use of commercial fertilizers ($\delta^{15}N$ range from -48.9 to $-19.9‰$, *Li and Wang* [2008]). However, only soil emissions and transport effects can cause the low $\delta^{15}N$ values observed in the ice cores.

Based on equation (6), the anthropogenic sources would have an associated $\delta^{15}N_{ant}$ value of 2.9‰, 2.5‰, and 2.7‰ for the United States, OECD Europe, and Russian Federation regions, respectively (Table 3). Transport isotope fractionation (ε) was estimated as -31.6 to $-31.9‰$ for the United States, OECD Europe, and Russian Federation regions (Table 3).

In equation (6), we have used the average value of $\delta^{15}N$ associated to both mobile and stationary sources (Table 3, row 1). However, recent studies by *Elliot et al*. [2007], *Elliot et al*. [2009], and *Redling et al*. [2013] have found that spatial patterns in $\delta^{15}N$ values are related to the contribution of NO_x emissions from stationary sources to NO_3^- deposition more than to vehicle emissions. Therefore, we have recalculated ε using only the average value of the $\delta^{15}N$ associated to NO_x emissions from public electricity and heat production (6‰ to 20‰, *Hastings* [2010, and references therein], and *Felix et al*. [2012]). Using only the stationary sources (Table 3, row 2), we calculate $\delta^{15}N_{ant}$ values of 6.0‰, 4.3‰, and 6.0‰ and —based on these— ε values of $-35‰$, $-33‰$, and $-35‰$ for the United States, OECD Europe, and Russian Federation regions, respectively (Table 3, row 10).

According to *Freyer et al*. [1993], variations in sample $\delta^{15}N$ values can be explained by the combination of changes in NO_x source strength and non-source-related processes (i.e., isotope fractionation during transport and kinetic or equilibrium reactions). Within the different non-source-related processes affecting the $\delta^{15}N$ values, the kinetic effects are especially tentative to point as causing the low $\delta^{15}N$ values observed in the LF-09 ice core. However, it should be mentioned that our simple isotope-mass balance model (equations (2)–(6)) does not account for possible temporal changes in the relevance of different non-source-related processes and considers those processes as constant during the time period covered by the LF-09 record. Consequently, our model emphasizes NO_x source strength variability to explain the temporal changes observed in the present isotopic data series.

When comparing the total NO_x emissions from the three main NO_x source regions assumed to influence the Arctic [*Felix and Elliot*, 2013]: United States, OECD Europe, and Russian Federation, between 1960 and 2008 [*van Aardenne et al*., 2001; *EC-JRC/PBL*. *EDGAR version 4.2*, 2011], with the NO_3^- quantified in the LF-97 [*Kekonen et al*., 2002], and LF-09, ice cores (Figures 8a and 8c), it is observed that the NO_3^- ice core data reproduces the higher emissions of NO_x during the 1970s and 1980s and their posterior decrease toward the 1990s. The total NO_x emissions are dominated by fossil fuel combustion, which are assumed to be one of that responsible for the transition from positive ice core $\delta^{15}N$ detected between preindustrial (pre-1900 LF-97 samples) and lower $\delta^{15}N$ in post-1950 samples (LF-09). In addition, it has been recently reported [*Felix and Elliot*, 2013] that the low ice core $\delta^{15}N$ values registered at Summit during the post-1920 period correlate with the increasing use of fertilizers over the United States. This suggests changes in NO_x sources, from biomass burning (plus lightning and other unknown natural sources) during preindustrial times, a combined biomass burning/fossil fuel source dominating the beginning of industrialization, to a biogenic source linked to the use of fertilizers over the last century is recorded as a decreasing trend in the $\delta^{15}N$ of NO_3^- in ice. This source scheme explains the trend observed by *Hastings et al*. [2009] for Greenland ice core data and also gives new insights in the combined NO_x sources that might be also recorded at Lomonosovfonna, with emphasis in fertilizers usage over Europe as responsible for the low $\delta^{15}N$ ice core values registered at Svalbard. A comparison of the LF-09 temporal $\delta^{15}N$ series and the three main NO_x source regions (United States, OECD Europe, and Russian Federation) is shown in Figures 8b–8e. As it can be observed in Figures 8b and 8d, there is a clear connection between the decrease of the $\delta^{15}N$ values and a steady increase in the U.S. soil emissions enhanced by fertilizer use during the last 50 years. This hypothesis is supported by the findings by *Samyn et al*. [2012], who mentioned the United States as one of the most important source regions for sulfate and NO_3^- found in Svalbard ice cores, followed by Western Europe. To reinforce this idea, Figures 8a, 8b, and 8f show the comparison between the ice core record and the N fertilizers consumption (International Fertilizer Industry Association (IFA), 2013, http://www.fertilizer.org, hereinafter referred to as IFA, online report, 2013) during the last 40 years in the three principal NO_x source

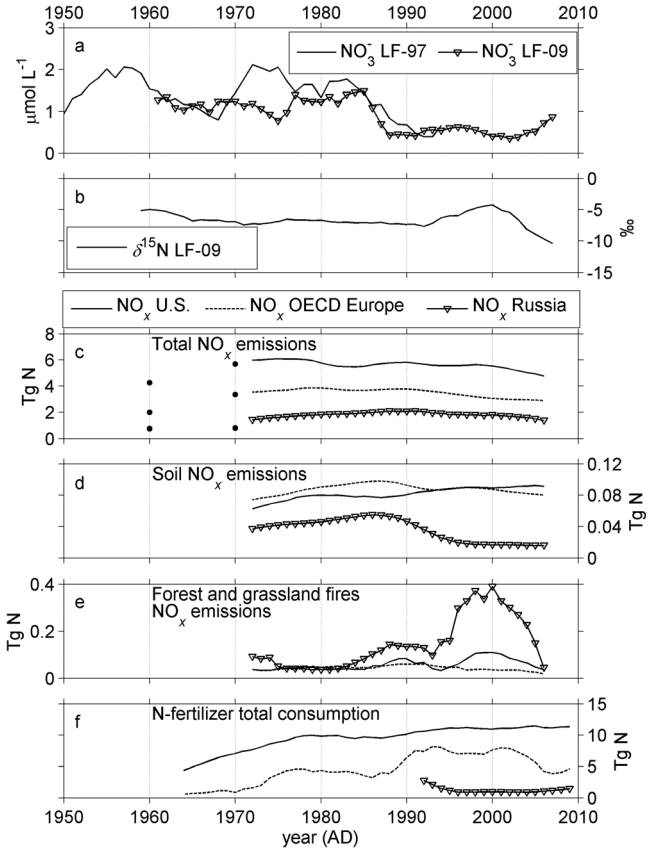

Figure 8. (a) NO_3^- concentrations measured in the LF-97 [*Kekonen et al.*, 2002] and LF-09, ice cores (solid and inverted triangle-line, respectively). (b) LF-09 δ^{15}N values. (c) Total NO_x emissions (dominated by fossil fuel and power plant combustion processes) [*EC-JRC/PBL. EDGAR version 4.2*, 2011] from the United States, OECD Europe, and Russia for the period between 1970 and 2008 (solid, dashed, and inverted triangle-line, respectively). Decadal NO_x emissions [*van Aardenne et al.*, 2001] were also included (black circle) to complete the time series back to 1960. Due to differences in the region classification between *van Aardenne et al.* [2001] and the *EC-JRC/PBL. EDGAR version 4.2.*, the NO_x emissions from Russia between 1970 and 2008 were completed using the Eastern Europe emissions between 1960 and 1970 [*van Aardenne et al.*, 2001]. (d) Soil, and (e) forest fires NO_x emissions from the three main source regions affecting Svalbard: the United States, OECD Europe, and Russia [*EC-JRC/PBL. EDGAR version 4.2*, 2011]. Note that the United States and OECD Europe NO_x emissions due to forest and grassland fires were scaled as 3 times the original value for better visualization. (f) N-fertilizer consumption in the three main NO_x source regions affecting Svalbard: the United States, OECD Europe, and Russia (IFA, online report, 2013). All data were smoothed using a 5 year moving average.

regions affecting Svalbard. As it can be observed in Figure 8f, N-based fertilizers consumption has increased in the last decades in Western Europe and the United States, which contributes to more productive soil, therefore enhancing soil NO_x emissions.

Correlation coefficients at the 95% confidence interval between fertilizer consumption and δ^{15}N (using 5 years moving averages of the data sets) between 1964 and 2007 were calculated and shown in Table 4. The *r* values show that considering the period 1964–2007, the δ^{15}N values do not reflect the effect of increasing fertilizer consumption (none of the correlations were significant at the 95% confidence interval). This is mainly due to the increase in δ^{15}N prior to the 1990s and reaching maximum values in 2000. However, if only the 1964–1990 period is considered, the *r* values reflect the influence of increasing fertilizer emissions leading to a decrease in δ^{15}N. The *r* values are higher when considering only U.S. fertilizer consumption (significant correlation at the 95% confidence interval), than when considering OECD Europe alone or combined with U.S. data (not significant).

To explain the increase in δ^{15}N in the ice core record observed around 2000 (Figure 4a), NO_x emission from forest and grassland fire activity is a possible alternative. *Hastings* [2010] has documented δ^{15}N aerosol values in the range of 10.6 to 25.7‰ after forest fires. As it can be observed in Figures 8b and 8e, there is a concomitant increase of δ^{15}N and NO_x emissions of Russian forest and grassland fires around 2000

Table 4. The *r* Values Calculated Between Fertilizer Consumption Data and δ^{15}N Values (All Data as 5 Year Moving Averages)[a]

r (1964–2007)	United States	OECD Europe	Russian Federation	(United States + OECD Europe)/2
δ^{15}N	0.004	0.29	−0.24	0.17
r (1964–1990)	United States	OECD Europe	Russian Federation	(United States + OECD Europe)/2
δ^{15}N	**−0.42**	−0.26	No overlapping	−0.35

[a]Significant *r* values ($p < 0.05$) were written in bold letters.

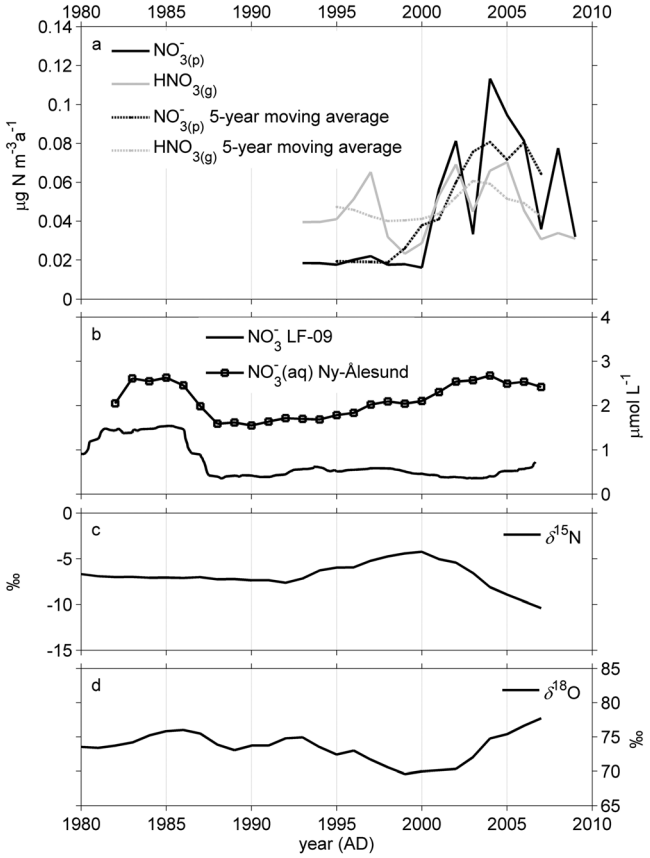

Figure 9. (a) Atmospheric data from Zeppelin station, Ny-Ålesund [*Aas et al.*, 2011]. Annual average $NO_{3(p)}^-$ (black line) and annual average $HNO_{3(g)}$ (grey line); the black and grey dashed lines indicates a 5 year moving average smoothing on the $NO_{3(p)}^-$ and $HNO_{3(g)}$ series, respectively. (b) Comparison between the LF-09 ice core NO_3^- concentrations (dashed line) and the NO_3^- measured in precipitation ($NO_{3(aq)}^-$) (black square-line) from Ny-Ålesund, Svalbard [*Aas et al.*, 2011]. (c) $\delta^{15}N$, and (d) $\delta^{18}O$ values measured in the LF-09 ice core. All data were smoothed using a 5 year moving average.

[*EC-JRC/PBL. EDGAR version 4.2*, 2011 http://edgar.jrc.ec.europa.eu/]. Similar increase can be observed in the U.S. emissions (note that the U.S. and OECD Europe NO_x emissions due to forest and grassland fires were scaled as 3 times the original value for better visualization in Figure 8e). Back-trajectory studies [*Eneroth et al.*, 2003; *Stohl*, 2006; *Stohl et al.*, 2007] have shown Siberia and Alaska as potential forest fire regions that affect the Arctic. Therefore, it is possible to connect the increase on $\delta^{15}N$ in the ice core with the increase in forest fire emissions during the early 2000s.

5.3. Comparison of the LF-09 NO_3^- Record With Ny-Ålesund Atmospheric Data and Other Arctic Sites

The LF-09 NO_3^- record was compared with nitrogen atmospheric data from Zeppelin Station, Ny-Ålesund, Svalbard (78°54'N, 11°53'E, 474 m asl), about 130 km NW of Lomonosovfonna, available at the EBAS database [*Aas et al.*, 2011]. Particulate NO_3^- measured in aerosol ($NO_{3(p)}^-$) and gaseous nitric acid present in the air ($HNO_{3(g)}$) were considered in this study. The $NO_{3(p)}^-$ and $HNO_{3(g)}$ daily series were reduced to annual averages between 1993 and 2009 and then smoothed with a 5 year moving average (Figure 9a). In addition, NO_3^- measured in precipitation samples from Ny-Ålesund ($NO_{3(aq)}^-$) [*Aas et al.*, 2011] were also considered between 1980 and 2009 (Figure 9b).

The comparison between the LF-09 NO_3^- data and the atmospheric data from Zeppelin ($NO_{3(p)}^-$ and $HNO_{3(g)}$) (Figures 9a and 9b), shows poor correlation between the ice core NO_3^- concentrations and the atmospheric data, for the period between 1993 and 2009 with $r(NO_{3(p)}^-|NO_3^-) = -0.016$ and $r(HNO_{3(g)}|NO_3^-) = -0.33$ at the 95% confidence interval, calculated using the 5 year moving average smoothed data.

When comparing the ice core NO_3^- concentrations with $NO_{3(aq)}^-$ (Figure 9b), the correlation coefficient has a value of $r(NO_{3(aq)}^-|NO_3^-) = 0.45$ for the period between 1980 and 2009. However, the correlation coefficient has a value of $r(NO_{3(aq)}^-|NO_3^-) = 0.86$ if just the period between 1980 and 2000 is considered, not including the post-2000 period where rapid changes in NO_3^- stable isotopes occurred (Figure 4). It is clearly seen in Figure 9b that the general patterns of $NO_{3(aq)}^-$ were registered in the LF-09 ice core, which is consistent with our correlation results.

On the other hand, the isotope deltas correlate better with the atmospheric data between 1993 and 2009 (Figures 9a, 9c, and 9d), with: $r(NO_{3(p)}^-|\delta^{15}N) = -0.73$, $r(HNO_{3(g)}|\delta^{15}N) = -0.34$, $r(NO_{3(p)}^-|\delta^{18}O) = 0.61$, and $r(HNO_{3(g)}|\delta^{18}O) = 0.25$ at the 95% confidence interval, calculated using the 5 year moving average smoothed data. This could indicate that the NO_3^- stable isotopic ratios depend more on the NO_3^- gas-particle relationship in the atmosphere than on the final deposited NO_3^- concentrations. It has been recently

Table 5. Correlation Coefficients (*r*) for Different Species Measured in the LF-09 Ice Core at the 95% Confidence Interval and Using the Time Series Smoothed Using a 5 Year Moving Average[a]

	1957–1990	1990–2009	
r	Period I	Period II	1957–2009
NO_3^-|NH_4^+	**0.50**	−0.12	**0.71**
NO_3^-|SO_4^{2-}	**0.45**	**0.95**	**0.82**
NH_4^+|SO_4^{2-}	**−0.47**	**−0.23**	**0.39**

[a]The *r* values were calculated for the whole core period 2009–1957, 2009–1990, and 1990–1957. The breakdown was chosen as 1990 where concentrations were stable after the fast decrease during the 1980s. Significant *r* values ($p < 0.05$) were written in bold letters.

described by *Geng et al*. [2014] that the decrease in δ^{15}N from Greenland ice cores registered over the industrial period might be related with a change in atmospheric acidity instead of a change in δ^{15}N from natural to anthropogenic sources. According to *Geng et al*. [2014], alterations of atmospheric acidity will lead to change the partition between $HNO_{3(g)}/NO_{3(p)}^-$ affecting the δ^{15}N signature in the ice. It has been previously mentioned that NO_3^- dry deposition contributes about ~14% of the total deposited NO_3^- in central Svalbard with $HNO_{3(g)}$ dry deposition being an order of magnitude higher than $NO_{3(p)}^-$ [*Björkman et al*., 2013]. Particulate NO_3^- would contribute about 1–7% of the total NO_3^- deposition [*Björkman et al*., 2013]. Our results show a better correlation between δ^{15}N and $NO_{3(p)}^-$ after 1993 than between δ^{15}N and $HNO_{3(g)}$. To explain the decreasing trend observed in the ice core δ^{15}N values toward the present, in terms of an increase in dry deposition, it is tempting to signal $NO_{3(p)}^-$ as the main trigger. However, its contribution to total deposited NO_3^- might not be enough to produce a significant change in the ice core δ^{15}N values; therefore, with the current knowledge available for Svalbard, this mechanism could not be pointed as responsible for the decreasing of the δ^{15}N during the last years.

A relatively low base line of nitrogen deposition ($NO_3^- + NH_4^+$) at Ny-Ålesund has been associated with frequent precipitation events [*Kühnel et al*., 2011], while high NO_3^- loads have been connected with sporadic precipitation events that are expected to be the result of fast and direct transport from low/middle latitudes into the Svalbard region. These strong events are more frequent during the winter season and show a high correlation coefficient between NO_3^- and NH_4^+. Fast and direct transport of air masses would result in less time for NO_x to undergo kinetic transformations, thus NO_x would not be intensity depleted in the ^{15}N isotope; therefore, it would be expected to keep the isotopic fingerprint of the dominant NO_x sources. There is a large interannual variability on these strong nitrogen deposition events and also spatial differences in depositional patterns [*Kühnel et al*., 2011], which increase the complexity of a direct comparison between the Zeppelin Station atmospheric data and the LF-09 ice core record. Table 5 shows the *r* values between NO_3^-, NH_4^+, and SO_4^{2-} species measured in the LF-09 ice core in order to assess the evidence of strong deposition events described by *Kühnel et al*. [2011]. Our results show that there is a high correlation between NO_3^--NH_4^+ ($r(NO_3^-|NH_4^+) = 0.71$ and NO_3^--SO_4^{2-} ($r(NO_3^-|SO_4^{2-}) = 0.82$) over the time span covered by the ice core (1957–2009). This suggests that the strong events detected by *Kühnel et al*. [2011] responsible for the NO_3^- loads over the Ny-Ålesund area might be also responsible for the NO_3^- input into the Lomonosovfonna ice cap. Moreover, when dividing the ice core time span between 1957–1990 (period I) and 1990–2009 (period II), the $r(NO_3^-|NH_4^+)$ values are 0.50 and −0.12, respectively, which can be interpreted as a change in the depositional patterns over Lomonosovfonna between periods I and II. It is also evident that NO_3^- correlates much better with sulfate than with ammonium during period II, which points to NO_3^- being codeposited with sulfate over the last 20 years more effectively than in period I.

Average stable isotope deltas and NO_3^- concentrations measured in the LF-09 and LF-97 cores are summarized in Table 2, along with snow and aerosol δ^{15}N and δ^{18}O data from Ny-Ålesund, Svalbard [*Heaton et al*., 2004; *Morin et al*., 2009; *Björkman*, 2013; *Björkman et al*., 2014], and ice core results for Summit [*Freyer et al*., 1996; *Hastings et al*., 2004, 2009]. Low and negative δ^{15}N values have been previously reported [*Heaton et al*., 2004] in snow samples (fresh snow and snow pack) collected in Ny-Ålesund during 2001–2003, with values at least (7–13)‰ lower than previously published NO_3^- data for snow and rain [*Heaton et al*., 2004]. Negative aerosol δ^{15}N values have also been reported at Ny-Ålesund [*Morin et al*., 2009], with mean values of (−15 ± 4)‰ during February to April 2006, together with other Arctic sites, such as Barrow and Alert, with values ranging from (−20.4 to −0.7)‰ and (−28.6 to −0.6)‰, for the two sites, respectively [*Morin et al*., 2012].

The LF-09 $\delta^{18}O$ results are in agreement with previous published data for low and polar latitudes [*Hastings et al*., 2004; *Morin et al*., 2009, 2012] measured in snow, rain and aerosol NO_3^- (Table 2). The preindustrial $\delta^{18}O$ values are in agreement with isotope deltas between (46.1 and 70.3)‰ measured in $NO_{3(p)}^-$ at Barrow [*Morin et al*., 2012], which points to similar oxidation pathways at both sites. However, three of four LF-97 samples that overlap with the LF-09 ice core showed 20 to 30‰ lower $\delta^{18}O$ values than the LF-09 samples (Figure 5). Potential analytical errors, as reason for the low $\delta^{18}O$ values, have been ruled out, since standards, reproducibility, and blank values were all normal during the analyses. We have also ruled out that isotopic exchange with water at some stage during storage, transport, or analysis of the samples, might have caused the low $\delta^{18}O$ values for the LF-97 samples since it has been recently estimated that the half-life for oxygen isotope exchange at natural conditions (25°C, pH 7) is in the order of 5.5×10^9 years [*Kaneko and Poulson*, 2013]. At the moment, we have not found an explanation to account for the low $\delta^{18}O$ values observed in the LF-97, considering that there is no apparent difference in the $\delta^{15}N$ or the NO_3^- concentrations between the LF-97 and LF-09 results.

6. Conclusions

It is evident from the LF-09 ice core record that the effect of anthropogenic sources is visible in the last decades and registered as low $\delta^{15}N$ values. We suggest that the NO_3^- stable isotopic signal recorded at Lomonosovfonna is influenced mainly by fossil fuel combustion, soil emissions, and forest fires; the first and second being responsible for the marked decrease in $\delta^{15}N$ between pre- and post-1950s, with soil emissions being associated to the decreasing trend in $\delta^{15}N$ registered toward the present and the latest being responsible for the sharp increase in $\delta^{15}N$ around 2000.

The results presented in this study suggest that the NO_3^- stable isotopic record from Lomonosovfonna describe the different sources of the NO_3^- found in the ice, either natural or anthropogenic. However, more knowledge on $\delta^{15}N$ and $\delta^{18}O$ fingerprints of NO_x sources, fractionation processes occurring during transport, local oxidation processes, and the snowpack NO_x emission effect on the ice core record at Lomonosovfonna, is needed to reinforce the NO_x source characterization from the ice core data. The currently limited knowledge regarding the processes of N_r fractionation within air masses traveling to polar regions, restrict us in exploring the signature of anthropogenic NO_x that may suffer ^{15}N depletion, causing the low values of $\delta^{15}N$ measured in the LF-09 ice core during the post-1950 period. We have evidence that fresh snow samples deposited at Ny-Ålesund by air masses backtracked to South–Easterly sources [*Björkman*, 2013; *Björkman et al*., 2014] have low $\delta^{15}N$, which reinforces the idea that the depletion of ^{15}N isotopes takes place during transport most probably due to kinetic fractionation.

The effects of local snow photochemistry emissions are ruled out as source of depleted snow $\delta^{15}N$, since photolysis will positively fractionate ^{15}N between the snow and the air. Moreover, low NO_x fluxes has been measured for Svalbard snow emissions during springtime [*Beine et al*., 2003; *Amoroso et al*., 2006; *Björkman*, 2013; *Björkman et al*., 2014], which implies that local production of HNO_3 from NO_x snowpack emissions, might not have a significant effect on the final ^{15}N depleted NO_3^- measured in the ice. The deposition of NO_3^- from air masses traveling over snow-covered areas that bare NO_3^- depleted in ^{15}N by photolysis, has been also ruled out as a contributor to the low $\delta^{15}N$ registered at Lomonosovfonna since most of the precipitation at this region occurs during autumn and winter when no photolysis takes place at this latitude and dry deposition of NO_3^- in Svalbard sites has been found low.

The results of this study represent the first data set of stable isotopes in NO_3^-measured in Svalbard ice cores, thus contributing and improving our understanding of the sources of nitrogen found in the High Arctic.

These first ice core NO_3^- stable isotopic records from Svalbard bring valuable complementary understanding of other proxy records for the Svalbard region, such as lake sediment cores. The quantification of NO_3^- stable isotopic signatures at different sites around Svalbard allows investigating their spatial variability and contributes to the understanding of NO_3^- sources and sinks in the Arctic region, and their effects on nitrogen-limited ecosystems.

Acknowledgments
The authors want to thank the drilling team and NPI field logistics for their support; M. Schwikowski and I. Wendl (both at the Paul Scherrer Institute, Switzerland) for their contribution on the ice core dating and ion chromatography support; and G. Engström (Uppsala University, Sweden) and S. Bejai (The Swedish University of Agricultural Sciences) for analytical lab facilities. Additionally, we thank the two anonymous reviewers for their valuable comments and suggestions, and J. Moore and C. Zdanowicz for insightful conversations. Volcanic Explosivity indexes were obtained from the Global Volcanism Program available at http://www.volcano.si.edu/#. Global and regional emissions of NO_x were obtained from the Emission Database for Global Atmospheric Research (EDGAR) at http://edgar.jrc.ec.europa.eu/ and http://themasites.pbl.nl/tridion/en/themasites/edgar/emission_data/edgar_32ft2000/documentation/index-2.html. Fertilizer consumption data were obtained from the International Fertilizer Industry Association (IFA) at http://www.fertilizer.org/ifa/ifadata/search. Ny-Ålesund Atmospheric data were obtained from the EBAS database operated by NILU at http://ebas.nilu.no. Lomonosovfonna ice core data (long ice core) were provided by M. Schwikowski (PSI). Previously reported Lomonosovfonna ice core data were provided by V. Pohjola and E. Isaksson. Original Lomonosovfonna ice core data shown here can be facilitated by C. P. Vega. This work was supported within the EU Marie Curie Initial Stage Training Network Award (NSINK, FP7 215503), with complementary economic support by NPI, Stiftelsen Ymer-80, and Geografiska Föreningen, Sweden. This is a contribution to Cryosphere-atmosphere interactions in a changing Arctic climate (CRAICC), a Top-level Research Initiative (TRI).

References

Aanes, R., B.-E. Sæther, and N. A. Øritsland (2000), Fluctuations of an introduced population of Svalbard reindeer: The effects of density dependence and climatic variation, *Ecography*, *23*(4), 437–443.

Aas, W., S. Solberg, S. Manø, and K. E. Yttri (2011), Overvåking av langtransportert forurenset luft og nedbør. Atmosfærisk tilførsel 2010, Kjeller, NILU (Statlig program for forurensningsovervåking. Rapport 1099/2011. TA-2812/2011) (NILU OR, 29/2011).

Amoroso, A., H. J. Beine, R. Sparapani, M. Nardino, and I. Allegrini (2006), Observation of coinciding arctic boundary layer ozone depletion and snow surface emissions of nitrous acid, *Atmos. Environ.*, *40*, 1949–1956.

Amoroso, A., et al. (2010), Microorganisms in dry polar snow are involved in the exchanges of reactive nitrogen species with the atmosphere, *Environ. Sci. Technol.*, *44*, 714–719.

Arthern, R. J., D. P. Winebrenner, and D. G. Vaughan (2006), Antarctic snow accumulation mapped using polarization of 4.3-cm wavelength microwave emission, *J. Geophys. Res.*, *111*, D06107, doi:10.1029/2004JD005667.

Atkin, O. K. (1996), Reassessing the nitrogen relations of Arctic plants: A mini-review, *Plant Cell Environ.*, *19*, 695–704.

Barrie, L. A. (1986), Arctic air pollution: An overview of current knowledge, *Atmos. Environ.*, *20*(4), 643–663.

Begun, G. M., and C. E. Melton (1956), Nitrogen isotopic fractionation between NO and NO_2 and mass discrimination in mass analysis of NO_2, *J. Chem. Phys.*, *25*(6), 1292–1293.

Beine, H. J., F. Dominé, W. Simpson, R. E. Honrath, R. Sparapani, X. Zhou, and M. King (2002), Snow-pile and chamber experiments during the Polar Sunrise Experiment 'Alert 2000': Exploration of nitrogen chemistry, *Atmos. Environ.*, *36*, 2707–2719.

Beine, H. J., F. Dominé, A. Ianniello, M. Nardino, I. Allegrini, K. Teinilä, and R. Hillamo (2003), Fluxes of nitrates between snow surfaces and the atmosphere in the European high arctic, *Atmos. Chem. Phys.*, *3*, 335–346.

Björkman, M. P. (2013), Nitrate dynamics in the arctic winter snowpack, Doctoral thesis, Akademika Publishing, Oslo, ISSN 1501–7710. Series of dissertations submitted to the Faculty of Mathematics and Natural Sciences, Univ. of Oslo, No. 1397.

Björkman, M. P., R. Kühnel, D. G. Patridge, T. J. Roberts, W. Aas, M. Mazzola, A. Viola, A. Hodson, J. Ström, and E. Isaksson (2013), Nitrate dry deposition in Svalbard, *Tellus B*, *65*, 19,071, doi:10.3402/tellusb.v65i0.19071.

Björkman, M. P., et al. (2014), Nitrate post-depositional processes in Svalbard surface snow, *J. Geophys. Res. Atmos.*, *119*, doi: 10.1002/2014JD021234.

Brown, L. L., and G. M. Begun (1959), Nitrogen isotopic fractionation between nitric acid and the oxides of nitrogen, *J. Chem. Phys.*, *30*(5), 1206–1209.

Burkhart, J. F., R. C. Bales, J. R. McConnell, and M. A. Hutterli (2006), Influence of North Atlantic Oscillation on anthropogenic transport recorded in northwest Greenland ice cores, *J. Geophys. Res.*, *111*, D22309, doi:10.1029/2005JD006771.

Casciotti, K. L., D. M. Sigman, M. G. Hastings, J. K. Böhlke, and A. Hilkert (2002), Measurement of the oxygen isotopic composition of nitrate in seawater and freshwater using the denitrifier method, *Anal. Chem.*, *74*, 4905–4912.

Coplen, T. B., J. K. Böhlke, and K. L. Casciotti (2004), Using dual-bacterial denitrification to improve $\delta^{15}N$ determinations of nitrates containing mass-independent ^{17}O, *Rapid Commun. Mass Spectrom.*, *18*, 245–250, doi:10.1002/rcm.1318.

Dibb, J. E., M. Arsenault, M. C. Peterson, and R. E. Honrath (2002), Fast nitrogen oxide photochemistry in Summit, Greenland snow, *Atmos. Environ.*, *36*, 2501–2511.

Dickson, L. G. (2000), INSTAAR constraints to nitrogen fixation by cryptogamic crusts in a polar desert ecosystem, Devon Island, N.W.T., Canada, *Arct. Antarct. Alp. Res.*, *32*(1), 40–45.

Divine, D., E. Isaksson, T. Martma, H. A. J. Meijer, J. Moore, V. Pohjola, R. S. W. van de Wal, and F. Godtliebsen (2011), Thousand years of winter surface air temperature variations in Svalbard and northern Norway reconstructed from ice-core data, *Polar Res.*, *30*, 7379, doi:10.3402/polar.v30i0.7379.

EC-JRC/PBL. EDGAR version 4.2 (2011), European Commission, Joint Research Centre (JRC)/Netherlands Environmental Assessment Agency (PBL), Emission Database for Global Atmospheric Research (EDGAR), release version 4.2. [Available at http://edgar.jrc.ec.europa.eu, 2011, Last Accessed: 12-08-2013.]

Elliot, E. M., C. Kendall, S. D. Wankel, D. A. Burns, E. W. Boyer, K. Harlin, D. J. Bain, and T. J. Butler (2007), Nitrogen isotopes as indicators of NO_x source contributions to atmospheric nitrate deposition across the Midwestern and northeastern United States, *Environ. Sci. Technol.*, *41*, 7661–7667.

Elliot, E. M., C. Kendall, E. W. Boyer, D. A. Burns, G. G. Lear, H. E. Golden, K. Harlin, A. Bytnerowicz, T. J. Butler, and R. Glatz (2009), Dual nitrate isotopes in dry deposition: Utility for partitioning NO_x source contributions to landscape nitrogen deposition, *J. Geophys. Res.*, *114*, G04020, doi:10.1029/2008JG000889.

Eneroth, K., E. Kjellström, and K. Holmén (2003), A trajectory climatology for Svalbard; investigating how atmospheric flow patterns influence observed tracer concentrations, *Phys. Chem. Earth*, *28*, 1191–1203.

Erbland, J., W. C. Vicars, J. Savarino, S. Morin, M. M. Frey, D. Frosini, E. Vince, and J. M. F. Martins (2012), Air-snow transfer of nitrate on the East Antarctic Plateau – Part 1: Isotopic evidence for a photolytically driven dynamic equilibrium, *Atmos. Chem. Phys. Discuss.*, *12*, 28,559–28,608, doi:10.5194/acpd-12-28559-2012.

Felix, J. D., and E. M. Elliot (2013), The agricultural history of human-nitrogen interactions as recorded in ice core $\delta^{15}N\text{-}NO_3^-$, *Geophy. Res. Lett.*, *40*, 1642–1646, doi:10.1002/grl.50209.

Felix, J. D., E. M. Elliot, and S. L. Shaw (2012), Nitrogen isotopic composition of coal-fired power plant NO_x: Influence of emission controls and implications for global emission inventories, *Environ. Sci. Technol.*, *46*, 3528–3535.

Fibiger, D. L., M. G. Hastings, J. E. Dibb, and L. G. Huey (2013), The preservation of atmospheric nitrate in snow at Summit, Greenland, *Geophys. Res. Lett.*, *40*, 3484–3489, doi:10.1002/grl.50659.

Fischer, H., D. Wagenbach, and J. Kipfstuhl (1998), Sulfate and nitrate firn concentrations on the Greenland ice sheet: 2. Temporal anthropogenic deposition changes, *J. Geophys. Res.*, *103*, 21,935–21,942, doi:10.1029/98JD01886.

Frey, M. M., J. Savarino, S. Morin, J. Erbland, and J. M. F. Martins (2009), Photolysis imprint in the nitrate stable isotope signal in snow and atmosphere of East Antarctica and implications for reactive nitrogen cycling, *Atmos. Chem. Phys.*, *9*, 8681–8696, doi:10.5194/acp-9-8681-2009.

Freyer, H. D. (1991), Seasonal variation of $^{15}N/^{14}N$ ratios in atmospheric nitrate species, *Tellus B*, *43*, 30–44.

Freyer, H. D., D. Kley, A. Volz-Thomas, and K. Kobel (1993), On the interaction of isotopic exchange processes with photochemical reactions in atmospheric oxides of nitrogen, *J. Geophys. Res.*, *98*, 14,791–14,796, doi:10.1029/93JD00874.

Freyer, H. D., K. Kobel, R. J. Delmas, D. Kley, and M. R. Legrand (1996), First results of $^{15}N/^{14}N$ ratios in nitrate from alpine and polar ice cores, *Tellus B*, *48*, 93–105.

Førland, E. J., R. Benestad, I. Hanssen-Bauer, J. E. Haugen, and T. E. Skaugen (2011), Temperature and precipitation development at Svalbard 1900–2100, *Adv. Meteorol.*, 893790, doi:10.1155/2011/893790.

Galloway, J. N., J. D. Aber, J. W. Erisman, S. P. Seitzinger, R. W. Howarth, E. B. Cowling, and B. J. Cosby (2003), The nitrogen cascade, *BioScience*, *53*(4), 341–356.

Geng, L., J. Cole-Dai, B. Alexander, E. J. Steig, A. J. Schauer, and J. Savarino (2014), Nitrogen isotopes in ice core nitrate linked to anthropogenic atmospheric acidity change, *Proc. Natl. Acad. Sci. U.S.A.*, *111*(16), 5808–5812.

Goto-Azuma, K., and R. M. Koerner (2001), Ice core studies of anthropogenic sulfate and nitrate trends in the Arctic, *J. Geophys. Res.*, *106*(D5), 4959–4969, doi:10.1029/2000JD900635.

Goto-Azuma, K., S. Kohshima, T. Kameda, S. Takahashi, O. Watanabe, Y. Fujii, and J. O. Hagen (1995), An ice-core chemistry record from Snøfjellafonna, northwestern Spitsbergen, *Ann. Glaciol.*, *21*, 213–218.

Hanna, E., J. McConnell, S. Das, J. Cappelen, and A. Stephens (2006), Observed and modeled Greenland ice sheet snow accumulation, 1958–2003, and links with regional climate forcing, *J. Clim.*, *19*(3), 344–358.

Hastings, M. G. (2010), Evaluating source, chemistry and climate change based upon the isotopic composition of nitrate in ice cores, *IOP Conf. Ser.: Earth Environ. Sci.*, *9*, 012002, doi:10.1088/1755-1315/9/1/012002.

Hastings, M. G., E. J. Steig, and D. M. Sigman (2004), Seasonal variations in N and O isotopes of nitrate in snow at Summit, Greenland: Implications for the study of nitrate in snow and ice cores, *J. Geophys. Res.*, *109*, D20306, doi:10.1029/2004JD00499.

Hastings, M. G., D. M. Sigman, and E. J. Steig (2005), Glacial/interglacial changes in the isotopes of nitrate from the Greenland ice sheet project 2 (GISP2) ice core, *Global Biogeochem. Cycles*, *19*, GB4024, doi:10.1029/2005GB002502.

Hastings, M. G., J. C. Jarvis, and E. J. Steig (2009), Anthropogenic impacts on nitrogen isotopes of ice-core nitrate, *Science*, *324*, 1288.

Heaton, T. H. E., P. Wynn, and A. M. Tye (2004), Low $^{15}N/^{14}N$ ratios for nitrate in snow in the High Arctic (79°N), *Atmos. Environ.*, *38*, 5611–5621.

Hirdman, D., H. Sodemann, S. Eckhardt, J. F. Burkhart, A. Jefferson, T. Mefford, P. K. Quinn, S. Sharma, J. Ström, and A. Stohl (2010), Source identification of short-lived air pollutants in the Arctic using statistical analysis of measurement data and particle dispersion model output, *Atmos. Chem. Phys.*, *10*, 669–693.

Holland, E. A., F. J. Dentener, B. H. Braswell, and J. M. Sulzman (1999), Contemporary and pre-industrial global reactive nitrogen budgets, *Biogeosciences*, *46*, 7–43.

Honrath, R. E., M. C. Peterson, S. Guo, J. E. Dibb, P. B. Shepson, and B. Campbell (1999), Evidence of NO_x production within or upon Ice particles in the Greenland snowpack, *Geophys. Res. Lett.*, *26*, 695–698, doi:10.1029/1999GL900077.

Honrath, R. E., S. Guo, M. C. Peterson, M. P. Dziobak, J. E. Dibb, and M. A. Arsenault (2000), Photochemical production of gas phase NO_x from ice crystal NO_3^-, *J. Geophys. Res.*, *105*(D19), 24,183–24,190, doi:10.1029/2000JD900361.

Isaksson, E., et al. (2001), A new ice-core record from Lomonosovfonna, Svalbard: Viewing the 1920–97 data in relation to present climate and environmental conditions, *J. Glaciol.*, *47*(157), 335–345.

Jarvis, J. C., E. J. Steig, M. G. Hastings, and S. A. Kunasek (2008), Influence of local photochemistry on isotopes of nitrate in Greenland snow, *Geophys. Res. Lett.*, *35*, L21804, doi:10.1029/2008GL035551.

Kahl, J. D. W., D. A. Martinez, H. Kuhns, C. I. Davidson, J.-L. Jaffrezo, and J. M. Harris (1997), Air mass trajectories to Summit, Greenland: A 44-year climatology and some episodic events, *J. Geophys. Res.*, *102*(C12), 26,861–26,875, doi:10.1029/97JC00296.

Kaiser, J., M. G. Hastings, B. Z. Houlton, T. Röckmann, and D. M. Sigman (2007), Triple oxygen isotope analysis of nitrate using the denitrifier method and thermal decomposition of N_2O, *Anal. Chem.*, *79*, 599–607.

Kaneko, M., and S. R. Poulson (2013), The rate of oxygen isotope exchange between nitrate and water, *Geochim. Cosmochim. Acta*, *118*, 148–156, doi:10.1016/j.gca.2013.05.010.

Kekonen, T., J. C. Moore, R. Mulvaney, E. Isaksson, V. Pohjola, and R. S. W. van De Wal (2002), A 800 year record of nitrate from the Lomonosovfonna ice core, Svalbard, *Ann. Glaciol.*, *35*, 261–265.

Kühnel, R., T. J. Roberts, M. P. Björkman, E. Isaksson, W. Aas, K. Holmén, and J. Ström (2011), 20-year climatology of NO_3^- and NH_4^+ wet deposition at Ny-Ålesund, Svalbard, *Adv. Meteorol.*, 406508, 10, doi:10.1155/2011/406508.

Laj, P., J. M. Palais, and H. Sigurdsson (1992), Changing sources of impurities to the Greenland ice-sheet over the last 250 years, *Atmos. Environ.*, *26*, 2627–2640.

Lamarque, J. F., et al. (2010), Historical (1850–2000) gridded anthropogenic and biomass burning emissions of reactive gases and aerosols: Methodology and application, *Atmos. Chem. Phys.*, *10*, 7017–7039, doi:10.5194/acp-10-7017-2010.

Li, D., and X. Wang (2008), Nitrogen isotopic signature of soil-released nitric oxide (NO) after fertilizer application, *Atmos. Environ.*, *42*, 4747–4754, doi:10.1016/j.atmosenv.2008.01.042.

Mayewski, P. A., W. B. Lyons, M. J. Spencer, M. S. Twickler, C. F. Buck, and S. Whitlow (1990), An ice-core record of atmospheric response to anthropogenic sulphate and nitrate, *Nature*, *346*(6284), 554–556.

Michalski, G., Z. Scott, M. Kabiling, and M. H. Thiemens (2003), First measurements and modeling of $\Delta^{17}O$ in atmospheric nitrate, *Geophys. Res. Lett.*, *30*(16), 1870, doi:10.1029/2003GL017015.

Moore, H. (1977), The isotopic composition of ammonia, nitrogen dioxide and nitrate in the atmosphere, *Atmos. Environ.*, *11*, 1239–1243.

Moore, J. C., E. Beaudon, S. Kang, D. Divine, E. Isaksson, V. A. Pohjola, and R. S. W. van de Wal (2012), Statistical extraction of volcanic sulphate from nonpolar ice cores, *J. Geophys. Res.*, *117*, D03306, doi:10.1029/2011JD016592.

Morin, S., J. Savarino, M. M. Frey, N. Yan, S. Bekki, J. W. Bottenheim, and J. M. F. Martins (2008), Tracing the origin and fate of NO_x in the arctic atmosphere using stable isotopes in nitrate, *Science*, *322*, 730–732.

Morin, S., J. Savarino, M. M. Frey, F. Domine, H.-W. Jacobi, L. Kaleschke, and J. M. F. Martins (2009), Comprehensive isotopic composition of atmospheric nitrate in the Atlantic Ocean boundary layer from 65°S to 79°N, *J. Geophys. Res.*, *114*, D05303, doi:10.1029/2008JD010696.

Morin, S., J. Erbland, J. Savarino, F. Domine, J. Bock, U. Friess, H.-W. Jacobi, H. Sihler, and J. M. F. Martins (2012), An isotopic view on the connection between photolytic emissions of NO_x from the Arctic snowpack and its oxidation by reactive halogens, *J. Geophys. Res.*, *117*, D00R08, doi:10.1029/2011JD016618.

Mosier, A. R., et al. (2002), Policy implications of human-accelerated nitrogen cycling, *Biogeosciences*, *57*/58, 477–516.

Pinglot, J. F., et al. (2003), Ice cores from Arctic sub-polar glaciers: Chronology and post-depositional processes deduced from radioactivity measurements, *J. Glaciol.*, *49*(164), 149–158.

Pohjola, V., T. Martma, H. A. J. Meijer, J. Moore, E. Isaksson, R. Vaikmäe, and R. S. W. van de Wal (2002), Reconstruction of three centuries of annual accumulation rates based on the record of stable isotopes of water from Lomonosovfonna, Svalbard, *Ann. Glaciol.*, *35*, 57–62.

Pohjola, V. A., J. C. Moore, E. Isaksson, T. Jauhiainen, R. S. W. van de Wal, T. Martma, H. A. J. Meijer, and R. Vaikmäe (2002), Effect of periodic melting on geochemical and isotopic signals in an ice core from Lomonosovfonna, Svalbard, *J. Geophys. Res.*, *107*(D4), 4036, doi:10.1029/2000JD000149.

Redling, K., E. Elliot, D. Bain, and J. Sherwell (2013), Highway contributions to reactive nitrogen deposition: Tracing the fate of vehicular NO_x using stable isotopes and plant biomonitors, *Biogeosciences*, *116*, 261–274, doi:10.1007/s10533-013-9857-x.

Rinnan, R., A. Michelsen, E. Bååth, and S. Jonasson (2007), Fifteen years of climate change manipulations alter soil microbial communities in a subarctic heath ecosystem, *Global Change Biol.*, *13*, 28–39, doi:10.1111/j.1365-2486.2006.01263.x.

Röthlisberger, R., et al. (2002), Nitrate in Greenland and Antarctic Ice cores: A detailed description of post-depositional processes, *Ann. Glaciol.*, *35*, 209–216.

Samyn, D., C. Vega, and V. A. Pohjola (2012), Nitrate and sulfate anthropogenic trends in the 20th century from five Svalbard ice cores, *Arct. Antarct. Alp. Res.*, *44*(4), 490–499, doi:10.1657/1938-4246-44.4.490.

Savarino, J., and S. Morin (2011), The N, O, S isotopes of oxy-anions in ice cores and polar environments, in *Handbook of Environmental Isotope Geochemistry*, vol. 39, pp. 835–864, Springer, New York, doi:10.1007/978-3-642-10637-8_39.

Savarino, J., J. Kaiser, S. Morin, D. M. Sigman, and M. H. Thiemens (2007), Nitrogen and oxygen isotopic constraints on the origin of atmospheric nitrate in coastal Antarctica, *Atmos. Chem. Phys.*, *7*, 1925–1945.

Shaver, G. R., and F. S. I. I. I. Chapin (1980), Response to fertilization by various plant growth forms in an Alaskan tundra: Nutrient accumulation and growth, *Ecology*, *61*(3), 662–675.

Stohl, A. (2006), Characteristics of atmospheric transport into the Arctic troposphere, *J. Geophys. Res.*, *111*, D11306, doi:10.1029/2005JD006888.

Stohl, A., et al. (2007), Arctic smoke–record high air pollution levels in the European Arctic due to agricultural fires in Eastern Europe in spring 2006, *Atmos. Chem. Phys.*, *7*, 511–534, doi:10.5194/acp-7-511-2007.

van Aardenne, J. A., F. J. Dentener, J. G. J. Olivier, C. G. M. Klein Goldewijk, and J. Lelieveld (2001), A 1° × 1° degree resolution data set of historical anthropogenic trace gas emissions for the period 1890– 1990, *Global Biogeochem. Cycles*, *15*(4), 909–928, doi:10.1029/2000GB001265.

van der Wel, L. G., H. J. Streurman, E. Isaksson, M. M. Helsen, R. S. W. van de Wal, T. Martma, V. A. Pohjola, J. C. Moore, and H. A. J. Meijer (2011), Using high resolution tritium profiles to quantify the effects of melt on two Spitsbergen ice cores, *J. Glaciol.*, *57*(206), 1087–1097.

Wagenbach, D., M. Legrand, H. Fischer, F. Pichlmayer, and E. W. Wolff (1998), Atmospheric near-surface nitrate at coastal Antarctic sites, *J. Geophys. Res.*, *103*(D9), 11,007–11,020, doi:10.1029/97JD03364.

Wendl, I., A. Eichler, L. Tobler, J. Eikenberg, T. Martma, E. Isaksson, E. Vogel, and M. Schwikowski (2011), First dating attempt for the 2009 ice core from Lomonosovfonna, Svalbard, *Labor für Radio- und Umweltchemie der Universität Bern und des Paul Scherrer Instituts Annual Report*, 41.